Preprints

2nd IFAC Workshop on Fractional Differentiation and its Applications

19 - 21 July, 2006
Porto, Portugal

IFAC

isep
Instituto superior de engenharia do porto

INSTITUTO POLITÉCNICO DO PORTO

FCT

Proceedings of the 2nd IFAC
Workshop on Fractional Differentiation and its Applications
Porto, Portugal, July 19-21, 2006

ANALYSIS OF FRACTIONAL - ORDER ROBOT AXIS DYNAMICS

J.M. Rosario[1], D. Dumur[2], J.A. Tenreiro Machado[3]

[1]Laboratory of Automation and Robotics - Faculty of Mechanical Engineering
UNICAMP - University of Campinas, 13083-970 – Campinas- SP, Brazil
rosario@fem.unicamp.br

[2]Department of Automatic Control
SUPELEC, 91192 - Gif-sur-Yvette, France
didier.dumur@supelec.fr

[3]Department of Electrical Engineering
Institute of Engineering, Polytechnic Institute of Porto, 4200-072, Porto, Portugal
jtm@isep.ipp.pt

Abstract: Robots are complex mechatronics systems where several electric drives are employed to control the movement of articulated structures. In industrial environments they must perform tasks with rapidity and accuracy in order to produce goods and services with minimal production time. These procedures require the use of flexible robots which can act in a large workspace, thus subjected to important parameters variations and nonlinear dynamics effects. This paper investigates the fractional order dynamics during the evolution of trajectories of three robotic joints, considering the complete system dynamics.

Keywords: Mechatronics, Robotics, Simulation, Dynamics, Control, Fractional calculus.

1. INTRODUCTION

The number of robots working in industry has increased significantly due to their operation capabilities in terms of flexibility, rapidity and accuracy. The integration of robots and mechatronic devices into a Flexible Manufacturing Cell (FMC) are essential to achieve this performance leading to a reduced production time and small energy consumption (David, et al. 1998; Pimenta, et al. 2001). Therefore, resourceful control algorithms must be implemented, which can cope with important parameters variations and vibration.

The study of feedback fractional order systems has been receiving considerable attention (Machado, 2003, Lima et al. 2005) both due to the fact that many physical systems are well characterized by fractional-order models, and with the success in the synthesis of fractional-order PID controllers that have been applied in a variety of dynamical processes (Barbosa, et al. 2004).

A Virtual Robot Environment was implemented that permits the analysis of the axis positions and velocities, electrical currents in the motors, and spatial displacement of this device. Therefore, the study presented here can assist in the design of the control system architecture to be used.

This paper presents a fractional system perspective in the study of the mechatronic device: a PRR robot with 3 DOF, as well as the dynamical modelling and simulation of this system, particularly emphasizing the development and implementation of robotic joint position controllers.

Bearing these ideas in mind, this paper is organized as follows. Section 2 describes the mechatronic system, including kinematics, dynamic and actuator modelling. Section 3 presents the axis control structure implemented under the RST form. Section 4 is dedicated to the results obtained within a virtual robotics environment. Finally, section 5 draws the main conclusions and points out future work.

2. MECHATRONIC SYSTEM

The mechatronic system is a FMC particular application based on the coordination and integration of two industrial robots and a PRR robot (prismatic-revolute-prismatic joints) developed for accurate welding work purposes (Fig.1). This device can assist in tasks for which traditional manipulators have difficulties to reach some parts of the piece. For that, the table is synchronized with the manipulators allowing them to carry out complex tasks without adjustments.

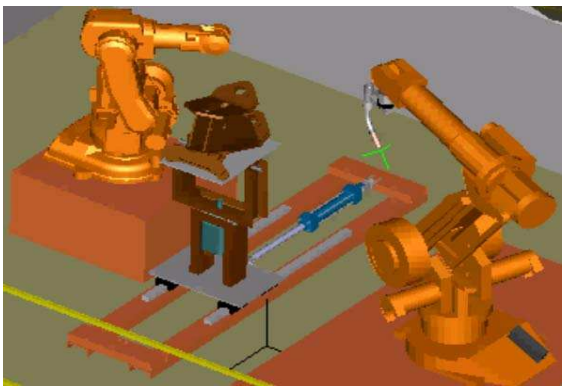

Fig. 1: Flexible Manufacturing Cell.

The modelling and simulation of the three degree-of-freedom (PRR robot), leads to the design of a virtual environment simulator adopting electric and mechanical libraries blocks using SIMULINK™.

The main elements of these robotics joints are brushless DC motor drives, axes inertia, gears and control blocks. Other elements of the manipulator (including loads) are represented by three nonlinear models, one for each motor drive.

The control system itself consists, essentially, in a cascade of control loops (for each axis). The inner speed and torque control loops are part of the drive model; only the position loop is explicitly modeled. In fact, the position control of the manipulator can be implemented through the control feedback of each isolated joint (David, et al. 1998), requiring the model of each joint.

The simulator also includes a path generation module, providing the joints with the axis trajectories as reference signals to the control parts. Finally, a graphical interface is available, showing results of joints movements obtained through typical trajectories.

2.1 Kinematics mode

The geometrical model of a 3 DOF robot provides the position $(p_x \;\; p_y \;\; p_z)$ and orientation $(\psi,\ \theta,\ \phi)$ with respect to a coordinate system fixed at the centre of the table, as a function of its generalized coordinates joints, that is:

$$\mathbf{x} = f(\boldsymbol{\theta}) \qquad (1)$$

where $\boldsymbol{\theta} = (d \;\; \theta_2 \;\; \theta_3)$ is the vector of joint positions and $\mathbf{x} = (p_x \;\; p_y \;\; p_z \;\; \psi \;\; \theta \;\; \phi)$ is the vector of the table positions.

Function *f* enables to calculate the movement of the end-effector resulting from the movement of the joints. This function is nonlinear and so (1) has a nontrivial analytical solution. This relation may be expressed mathematically by a matrix connecting the system of fixed coordinates in the base of the robot with a system of coordinates associated to the robot. This matrix, the so called homogeneous transition matrix, is obtained through the product of the homogeneous transformations matrix $\mathbf{A}_{i,i-1}$, linking the system of coordinates of element i with the system of the previous element $i-1$, that is:

$$\left[\mathbf{n}^{\mathrm{T}} \;\; \mathbf{s}^{\mathrm{T}} \;\; \mathbf{a}^{\mathrm{T}} \;\; \mathbf{p}^{\mathrm{T}}\right] = \mathbf{T}_n = \mathbf{A}_{0,1}\,\mathbf{A}_{1,2}\,\mathbf{A}_{2,3} \qquad (2)$$

where $\mathbf{p} = [p_x \;\; p_y \;\; p_z]$ is the position vector and $\mathbf{n} = [n_x \;\; n_y \;\; n_z]$, $\mathbf{s} = [s_x \;\; s_y \;\; s_z]$, $\mathbf{a} = [a_x \;\; a_y \;\; a_z]$ represent the orientation vector.

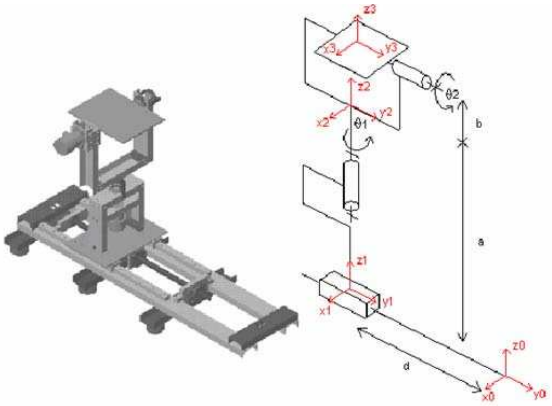

Axis	α_i	d_i	θ_i	r_i
1	0	*d*	0	0
2	0	0	θ_2	*a*
3	θ_3	0	0	*b*

Fig. 2: PRR robot - Denavit-Hartenberg parameters.

The kinematics description of this robot is performed through the Denavit-Hartenberg procedure, after isolating the four parameters $\{\boldsymbol{\theta}_i, \mathbf{r}_i, \mathbf{d}_i, \boldsymbol{\alpha}_i\}$ (Fig. 2). These coefficients enable representing the different positions of the parts of this mechanical device. The position vector $(p_x \;\; p_y \;\; p_z)$ and the orientation angles $(\psi \;\; \theta \;\; \phi)$ for an object with dimensions $(L_x \;\; L_y \;\; L_z)$ placed in the centre of the table are given by:

$$\begin{aligned} p_x &= L_x\, c_2\, c_3 - L_y\, s_1 + L_z\, c_2\, s_3 \\ p_y &= L_x\, s_2\, c_3 + L_y\, c_2 + L_z\, s_2\, s_3 + d \\ p_z &= -L_x\, s_2 + L_z\, c_2 + (a + b \end{aligned} \qquad (3)$$

$$(\psi\ \ \theta\ \ \phi) = \mathrm{rot}(x,\phi)\mathrm{rot}(y,\theta)\mathrm{rot}(z,\psi)$$

$$= \begin{bmatrix} c\phi\ c\theta & -c\phi\, s\theta\, s\psi - s\phi\, c\psi & c\phi\, s\theta\, c\psi + s\phi\, s\psi \\ s\phi\ c\theta & -s\phi\, s\theta\ s\psi + c\phi\, c\psi & s\phi\, s\theta\, c\psi - c\phi\, s\psi \\ -s\theta & c\theta\, s\psi & c\theta\, c\psi \end{bmatrix} \quad (4)$$

$$\theta = ATAN2\left[\frac{-n_Z}{c\phi\, n_x + s\phi\, n_y}\right],\ \phi = ATAN2\left[\frac{n_y}{n_x}\right]$$

$$\psi = ATAN2\left[\frac{s\varphi\, a_x - c\varphi\, a_y}{-s\varphi\, s_x + c\varphi\, s_y}\right]$$

$$n_x = c_2 \qquad n_y = s_2 \qquad n_z = 0$$

$$s_x = -s_2\, c_3 \quad s_y = c_2\, c_3 \quad s_z = s_3$$

$$a_x = s_2\, s_3 \quad a_y = -c_2\, s_3 \quad a_z = c_3$$

$$c_i = \cos\theta_i \quad s_i = \sin\theta_i \quad \text{(likewise for } \theta,\ \phi, \psi)$$

where the function ATAN2 to mean that the arc of tangent is reckoned according to an algorithm talking into account that the values of both sine and cosine are known, and hence the quadrant of the angle may be deduced.

The elaboration of references in angular coordinates, referring to the tasks defined in the Cartesian space, is expressed mathematically by the numerical inversion of the kinematics model using the Jacobian function, which is:

$$\Delta\boldsymbol{\theta} = J^{-1}(\theta)\Delta\mathbf{x} \quad (5)$$

2.2 Control structure including kinematics

For many operations the operator defines the tasks, or reference trajectories of the controller, in relation to a coordinate system that is fixed to the end-effector of the robot (in the Cartesian space). Nevertheless, the desired movements (expressed in angular coordinates) and the control laws are in different coordinate systems, requiring the implementation of algorithms for the inversion of the kinematics model and the generation of the reference trajectory in angular coordinates. In this way, its trajectory is defined through a set of angles associated to the angular movement of each degree of freedom of the robot. After interpolation, these angles will act as reference signals for positioning controllers located at each joint, that compare the signals deriving from the position sensors of the joints (Pimenta, et al 2001).

2.4 Actuator model

Each robotic joint commonly includes a DC motor, a gear and an encoder. Considering the DC motor, the three classical equations are the following:

$$u(t) = L\frac{\mathrm{d}\, i(t)}{\mathrm{d}\, t} + R\, i(t) + K_E\frac{\mathrm{d}\,\theta_m(t)}{\mathrm{d}\, t}$$

$$T_m(t) = J_{eq}\frac{\mathrm{d}^2\,\theta_m(t)}{\mathrm{d}\, t^2} + B_m\frac{\mathrm{d}\,\theta_m(t)}{\mathrm{d}\, t} \quad (7)$$

$$T_m(t) = K_T\, i(t)$$

where $T_m(t)$ is the motor torque, $\theta_m(t)$ the angular position of the motor, $i(t)$ the motor current, L, R respectively the inductance, resistance of the motor, J_{eq} the inertia of axis load calculated on the motor side, resulting in the block diagram of Fig. 3.

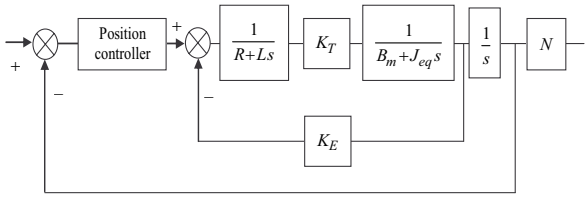

Fig. 3: Block diagram of the joint axis.

2.3 Dynamic model

As previously mentioned, the control of each joint is considered independently. To take coupling effects into account, and to solve the trajectory problem, the dynamic control involves the determination of the inputs, so that the drive of each joint moves its links to the position values with the required speed. The dynamic model of a robotic joint can be derived through the Euler-Lagrange formulation that expresses the generalized torque (David, et al 1998). The manipulator dynamic behavior is described by a group of differential equations called dynamic equations of motion. For an N DOF rigid manipulator, the equations are:

$$\tau_i(t) = J_i(\theta(t))\,\ddot{\theta}_i(t) + C_i(\theta\, t\ ,\dot{\theta}\ t\ ) + Q_i(\theta(t)) \qquad i = 1,\cdots,3 \quad (6)$$

where $\tau_i(t)$ is the generalized torque vector, $\theta_i(t)$ the generalized frame vector (joints), $J_i(t)$ the inertial matrix, $C_i(\theta,\dot{\theta})$ the non-linear forces (for example centrifugal) matrix, $Q_i(\theta)$ the gravity force matrix. Fig. 4 shows the complete dynamical model considering for analysis, 2 robotic axes only.

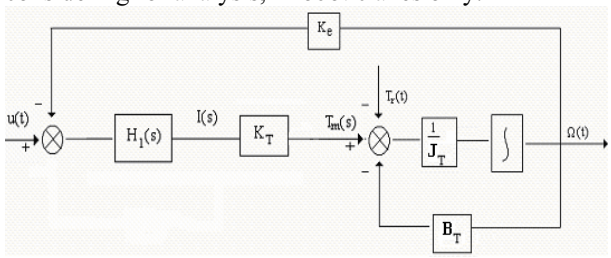

Fig. 4: Transfer Function and Dynamical Model.

$$J_{T1}\ddot{\theta}_1 + B_{T1}\dot{\theta}_1 + T_{r1} = T_{m1} \qquad J_{T2}\ddot{\theta}_2 + B_{T2}\dot{\theta}_2 + T_{r2} = T_{m2}$$

with

$$J_{T1} = A_2 + K_1 + A_3 c\theta_1,\ B_{T1} = -A_3\dot{\theta}_2\, s\theta_2$$

$$T_{r1} = (A_3 + \frac{1}{2}A_2 c\theta_2)\ddot{\theta}_2 + (-\frac{1}{2}A_2\dot{\theta}_2^{\,2}\, s\theta_2) + A_4 c\theta_1 + A_5 c(\theta_1+\theta_2)$$

$$J_{T2} = A_3\ ,\ B_{T2} = 0$$

$$T_{r2} = (A_3 + \frac{1}{2}A_2 c\theta_2)\ddot{\theta}_1 + \frac{1}{2}A_2\dot{\theta}_1^{\,2}\, s\theta_2 + A_5 c(\theta_1+\theta_2)$$

The controller makes the corrections taking into account the robot's dynamic model developed above. These corrections are transmitted to the manipulator through the actuator described in the next subsection, including a gearbox characterized by their ratio, inertia and stiffness and damping of input and output shafts. The gearboxes' output shafts are connected to the other parts of the robot structure, which results in the effective torque reflected to each joint. For each of the three joints, the other links effects are globally considered as a single load inducing to the joint a torque composed of three terms (Eq. 6).

3. AXIS CONTROL ARCHITECTURE

One advantage of the virtual environment is the possibility to implement and test advanced axis control strategies, in particular Predictive Control, a well known structure providing improved tracking performances. This philosophy aiming at creating an anticipative effect is using the explicit knowledge of the trajectory in the future (Boucher, et al 1995).

3.1 RST form of the controller

The minimization of the cost function results in the predictive controller derived in the RST form according to Fig. 5 and implemented through a difference equation:

$$S(q^{-1})\Delta(q^{-1})u(t) = -R(q^{-1})y(t) + T(q)w(t) \quad (11)$$

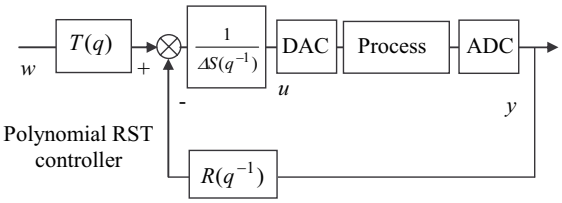

Fig. 5: GPC in a RST form.

The main feature of this RST controller is the non causal form of the T polynomial, creating the anticipative effect of this control law.

4. TESTS IN THE VIRTUAL ENVIRONMENT

Previous sections have described the whole virtual environment related to the 3 DOF manipulator, including motor drives, gear boxes, kinematic and dynamic models, and predictive axis controllers, designed with electric drives and SIMULINK™ libraries. This section will now present results obtained within this environment. Simulations described below consider 3D trajectories issued from the path generation module.

4.1 Actuator parameters

The system considered here, used for supervision and control, includes three DC motors, a 1:100 gear box, a ball screw transmission (only for axis 1) and incremental encoders (Table 1).

Table 1: Motor Parameters.

Inertia (kgm2)	**0.71 10-3**
Weight (kg)	**8**
Mechanical time constant (ms)	**1.94**
Voltage constant (V/rad/s)	**0.807**
Torque constant (Nm/A)	**1.33**
Inductance (mH)	**14.7**
Resistance (Ω)	**1.44**

4.2 GPC tuning parameters

The axis controllers are designed independently following the mechanism developed resulting in three RSTs, considering the same axis motor but with different inertia on the motor side due to different geometrical features for each axis (Fig.6).

Four tuning parameters are required: N_1 the minimum prediction horizon, N_2 the maximum prediction horizon, N_u the control horizon and λ the control weighting factor. The parameters given in Table 2 have been chosen to provide good stability and robustness margins (Boucher, et al. 1995).

Table 2: GPC tuning parameters for each joint.

Axis	N_1	N_2	N_u	λ
1	**1**	**8**	**1**	**92**
2	**1**	**8**	**1**	**107.3**
3	**1**	**8**	**1**	**126**

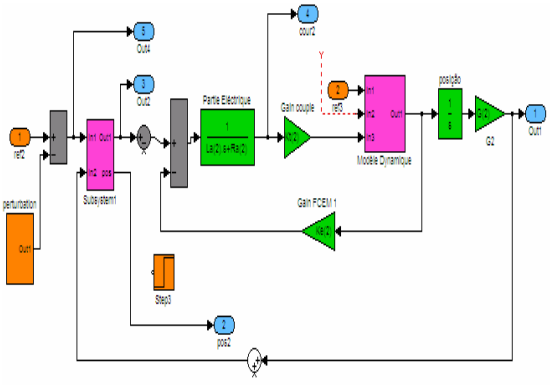

Fig. 6: Simulink Diagram of joint control (1 axe).

4.3 Simulation scenario

The scenario considers the rotational trajectory around the z-axis followed by a rod of 100 mm length (L), located at the center of the table of the 3 axis robot, with a 30° inclination angle. To do that, the second and third axes are operating with maximal and 10% velocity respectively.

During the movement, small disturbances are added at the axis 2 reference signal at the time interval between 3s - 3.5s, with amplitude level, in order of the 10% of maximal current.

The desired path is thus a revolution cone considering the dynamical model of axes, as shown in Fig. 7. The effects of disturbances on each joint can be seen. The several signals are recorded with a sampling frequency of f_s = 10 KHz.

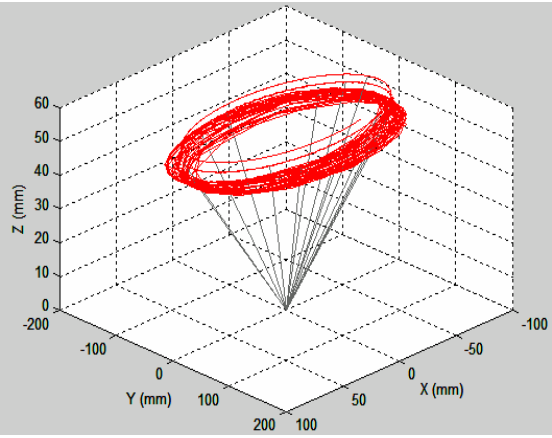

Fig. 7: Spatial trajectory.

4.4 Simulation results

The simulation results obtained using axis controllers, considering a disturbance effects and the error analysis between previous scenarios. The fractional analysis is realized using the Fast Fourier Transform (FFT), using the transfer function, between the reference signal and motor current. For analysis the difference of this signals is used, considering without and with disturbances effects applied at axis 2.

Fig. 8 shows the amplitude of the Fast Fourier Transform (FFT) of the axis 2 motor current signal. The spectrum was also approximated by trend lines in a frequency range larger than a decade. Table 3 presents the main results obtained for 3 robotic joints by fitting parameters using a power function type $|I_2(f)| = a f^b$, $a,b \in \Re$, with frequency range f1.

4.5 Simulation analysis

Tracking performances offered by GPC laws presents very small tracking errors at the trajectories evolution. Globally, the results shows that the anticipative effect of the GPC law can provide better performances, even if the controllers were designed neglecting the coupling effect between each axis. In this direction, GPC is less sensitive to inertia variations (appearing as every axis acts on the other ones) than PID. This significant simulation shows the robustness of GPC, so that the inertia variation can be considered as a disturbance performing on the system.

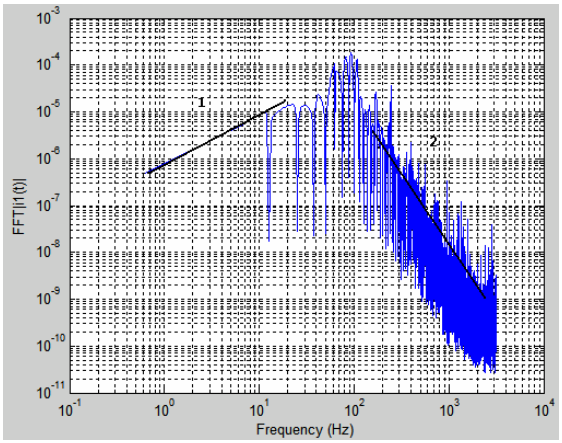

a) Joint 1.

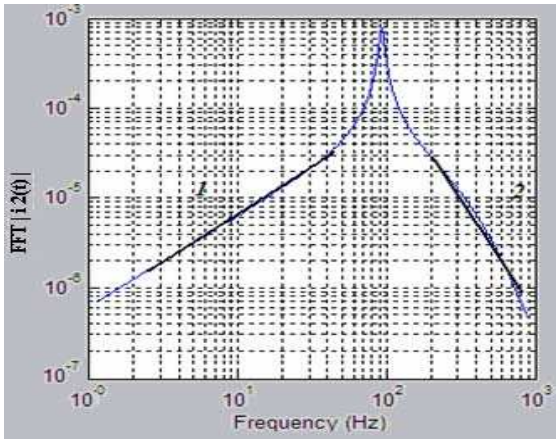

b) Joint 2.

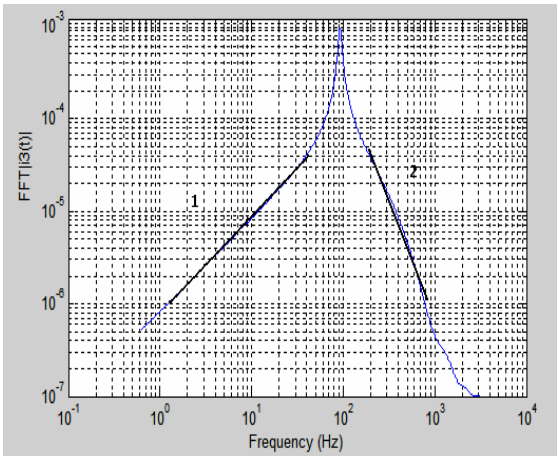

c) Joint 3

Fig. 8: Spectrum results for 3 axis motor current.

The results of Fig. 8 and table 3 shows part 1of | i(*f*) | for each robotic joint with a trend line superimposed over the signal, with slope approximately b = 1.06, that reveals, clearly, an integer order behavior. Similarly, part 2 of the spectrum signal was also approximated by a trend line in a frequency range larger than a decade, with a slope approximately of b = –3.3 presenting, clearly, a fractional order behavior. Other important transfer functions involved other robot axis coupling were studied, revealing also an integer behavior, but under disturbance and no disturbance.

The 2 and 3 axis motor current for a limited frequency range present also fractional order behavior while the joint 1 the spectrum is not defined in a large frequency range, because he has dynamic effects occurred because the coupling between axis.

The position signals were studied, revealing also an integer behavior, both under disturbance and no disturbance conditions.

Table 3: Fitting Parameters of FFT$|i(t)| = a f^b$.

Joint 1

Freq. (Khz)	*A*	*B*	R^2
0 < f1 < 0.15	2,269E-06	1,053	9,9400E-01
0.3 < f2 < 0.8	1,177E+04	-3,310E+00	9,99300E-01

Joint 2

Freq. (Khz)	*A*	*B*	R^2
0 < f1 < 0.15	2,272E-06	1,061	9,9978E-01
0.3 < f2 < 0.8	1,167E+04	-3,310E+00	9,9972E-01

Joint 3

Freq. (Khz)	*A*	*B*	R^2
0 < f1 < 0.15	2,271E-06	1,059	9,9998E-01
0.3 < f2 < 0.8	1,173E+04	-3,340E+00	9,9997E-01

5. CONCLUSIONS AND FURTHER WORKS

In this paper a study was conducted to investigate several robot signals, in a fractional system perspective using a Virtual Robot Environment and the case study for a 3 DOF manipulator. For that purpose, a complete modular virtual environment was designed using SIMULINK™ framework. This simulator includes the kinematics and dynamic models as well as the axis controlled loops built around the actuator model, i.e. DC motor with gear box and ball screw for the translational joint. A trajectory generation module and a graphical interface were developed to help the user in testing realistic manipulator configurations. To emphasize the modularity of this virtual environment, electrical drive and controller libraries were integrated as well; additional user-defined plug-in modules can be added very easily.

In this direction, the axis controllers were structured under the RST formalism, which corresponds to the generic framework for numerical control. From this form, a GPC control law was implemented on each axis, simply designed without taking into account coupling effects, providing improved performances in terms of rapidity, cancellation of overshoot, accuracy, disturbance rejection and robustness towards inertia variations and non linearities. This last point is one of the main challenges of robot control, mainly when large workspace is involved, because inertia can present important variations. For comparison with a classical control axis strategy., the GPC controller has shown to be an effective strategy in many fields of applications, with good time-domain and frequency properties (small overshoot, improved tracking accuracy and disturbance rejection ability, good stability and robustness margins), able to cope with important parameters variations.

The study provides useful information that can assist in the design of a control structure to be used in eliminating or reduction the dynamical coupling between joints. Further work will look at the robustness of the GPC strategy against measurement noise and parameters uncertainties, as well as real validation of the developed control algorithms accomplished through an experimental implementation.

6. ACKNOWLEDGEMENT

The authors acknowledge support of the Brazilian Research Council - CAPES"- Brazil, through a collaborative work between the ISEP, Portugal and UNICAMP, Brazil and ARCUS cooperation program with SUPELEC, France.

REFERENCES

Barbosa, R.S., Tenreiro Machado, J.A., Ferreira, I.M. (2004). Tuning of PID Controllers Based on Bode's Ideal Transfer Function, *Nonlinear Dynamics 38*, pp. 305-321, Kluwer Academic Publishers.

Boucher, P., Dumur, D. (1995), Predictive Motion Control, *Journal of Systems Engineering, Special Issue on Motion Control Systems*, 5: pp.148-162, Springer-Verlag.

Clarke, D.W., Mohtadi, C., Tuffs, P.S. (1987), Generalized Predictive Control, Part I "The Basic Algorithm", Part II "Extensions and Interpretation, *Automatica,* 23(2):137-160.

David, S., Rosário, J.M. (1998), Modeling, Simulation and Control of Flexible Robots, *CONTROLO'98*, pp. 532-539, Coimbra, Portugal .

Lima, M.F.M., Tenreiro Machado, J.A. (2005). Experimental Set-Up for Vibration and Impact Analysis in Robotics, *WSEAS Trans. on Systems*, Issue 5, vol. $, May, pp. 569-576.

Pimenta, K.B., Souza, J.P., Rosário, J.M., Dumur, D. (2001), Control of Robotic Joints with Generalized Predictive Control (GPC), *RADD'2001*, Vienna, Austria.

Tenreiro Machado, J.A. (2003), A Probabilistic Interpretation of the Fractional-Order Differentiation, *Journal of Fractional Calculus & Applied Analysis*, vol. 6, No 1, pp. 73-80.